Single ODSB Radio-Over-Fiber Signal Supports STBC at Each RAP

Varghese Antony Thomas, Mohammed El-Hajjar, and Lajos Hanzo

***Abstract*—We propose and mathematically characterize a novel radio-over-fiber (ROF) downlink, where a radio access point (RAP) benefits from the transmit diversity gain of space–time block coding (STBC). Significantly, this transmit diversity is achieved using a single optical modulator in the base station (BS). In the proposed architecture, each RAP is fed with a single optical double-sideband signal, where each sideband transmits one of the two STBC-encoded signals. This optical signal is generated in the BS by performing the simultaneous optical upconversion of the baseband STBC signals using a single Mach–Zehnder modulator. The proposed optical backhaul is designed and simulated to impose negligible degradation to that imposed by the dominant wireless link, thereby enabling a designer to exploit the advantages offered by a wireless link having a diversity gain.**

***Index Terms*—Author, please supply index terms/keywords for your paper. To download the IEEE Taxonomy go to http://www.ieee.org/documents/taxonomy_v101.pdf.**

I. Introduction

THE optical-wireless backhaul technique of ROF makes a network employing small cells and high-RF carriers cost-effective. Each cell of a ROF-aided network is served by a RAP, while multiple RAPs are connected to a central BS via optical fiber [1]–[3]. Centralized signal processing at the BS *simplifies* the RAP and hence facilitates cost reduction [4]–[6].

A. Motivations for the Proposed Architecture

Some important challenges *of* large-scale employment of ROF-aided high-RF systems *are as follows.*

1. Electronic components, especially the mixers, exhibit a degraded performance at high frequencies [4]. Optical generation of the RF signal is a potential solution to this challenge [7]. For example, [8] is a recent paper that proposes a new method for optical generation of UWB RF signals.
2. Multiple input multiple output (MIMO) techniques like the classic STBC devised by Almouti in [9] *can* be employed in the wireless link of ROF systems *to improve* the downlink bit error rate (BER) performance [10], [11]. However, multiple optical modulators may be required at the central BS for supporting MIMO transmission from each RAP as in [10].
3. The most commonly employed ODSB modulation, unlike the optical single side band (OSSB) modulation, is severely affected by the chromatic dispersion-induced power attenuation at high RF carriers [12].

Manuscript received November 3, 2014; revised March 10, 2015 and April 30, 2015; accepted May 1, 2015. The associate editor coordinating the review of this paper and approving it for publication was J. Cheng.

The authors are with the School of Electronics and Computer Science, University of Southampton, Southampton SO17 1BJ, U.K. (e-mail: vat1g10@ecs.soton.ac.uk; meh@ecs.soton.ac.uk; lh@ecs.soton.ac.uk).

Digital Object Identifier 10.1109/LCOMM.2015.2429574

B. Advantages of the Proposed Architecture

The proposed architecture implements optical upconversion to avoid the use of electronic mixers [7]. Optical upconversion is implemented using a MZM driven by a sawtooth signal. Both sidebands of the classical ODSB carry the same signal [13]. In contrast to *the classical ODSB*, the optical signal generated in the proposed architecture is an ODSB signal in which the two sidebands transmit two different signals, namely the two STBC-encoded signals. Thus, a single dual-drive MZM supports 2×1 STBC Transmission from each RAP, thereby addressing the second challenge discussed in Section I-A In the RAP, the two sidebands are separately photo-detected, which gives it the performance advantages of an OSSB signal, thereby addressing the final challenge discussed in Section I-A. Each RAP has a pair of antennas. The two photo-detected signals are transmitted to the mobile station (MS) using different antennas, where the MS has a STBC receiver.

II. Proposed Downlink Architecture and Analysis

A. Transmitter in the BS

The laser diode (LD) in the BS of Fig. 1(a) has an optical frequency of f_c Hz and a power of P_{LD}, while its optical output field is [5], [13]

$$E_{LD}(t) = \sqrt{2P_{LD}}e^{j2\pi f_c t}. \tag{1}$$

As shown in Fig. 1(a), the output of the laser is split by a 3 dB optical power splitter having an insertion loss of t_{sp} to yield

$$E_{c,1}(t) = E_{c,2}(t) = \sqrt{\frac{t_{sp}}{2}}E_{LD}(t). \tag{2}$$

The optical signal $E_{c,1}(t)$ is fed to a dual-drive MZM with its arms driven by signals $v(t) + x_1^{STBC}(t)$ and $-v(t) - x_2^{STBC}(t)$. If $x(t)$ is the baseband signal with bit-rate R_{bit} to be transmitted over the wireless link to the MS using RF phase modulation, then $x_1^{STBC}(t)$ and $x_2^{STBC}(t)$ are generated from $x(t)$ such that $e^{j(\pi \frac{x_1^{STBC}(t)}{V_\pi})}$ and $e^{j(\pi \frac{x_2^{STBC}(t)}{V_\pi})}$ are the STBC symbols transmitted to the MS [9]. If $x(t)$ consists of $2N$ symbols $\{x_k | 1 < k < 2N\}$, then, for $1 < i < N$, the $(2i-1)^{th}$ and $(2i)^{th}$ symbols of the STBC signals are given by the first and second rows of the following matrix, respectively

$$\begin{bmatrix} e^{j\left(\pi \frac{x_1^{STBC}}{V_\pi}\right)} & e^{j\left(\pi \frac{x_2^{STBC}}{V_\pi}\right)} \end{bmatrix} = \begin{bmatrix} e^{j\left(\pi \frac{x_{2i-1}}{V_\pi}\right)} & e^{j\left(\left(\pi \frac{x_{2i}}{V_\pi}\right)\right)} \\ -\left(e^{j\left(\pi \frac{x_{2i}}{V_\pi}\right)}\right)^* & \left(e^{j\left(\pi \frac{x_{2i-1}}{V_\pi}\right)}\right)^* \end{bmatrix}.$$

On the other hand, $v(t)$ is a sawtooth-shaped function given by

$$v(t) = modulo[2f_{rf}tV_\pi, 2V_\pi] - V_\pi \tag{3}$$

where f_{rf} is the RF carrier transmitted from the RAP to the MS, while V_π is the switching voltage of the dual-drive MZM.

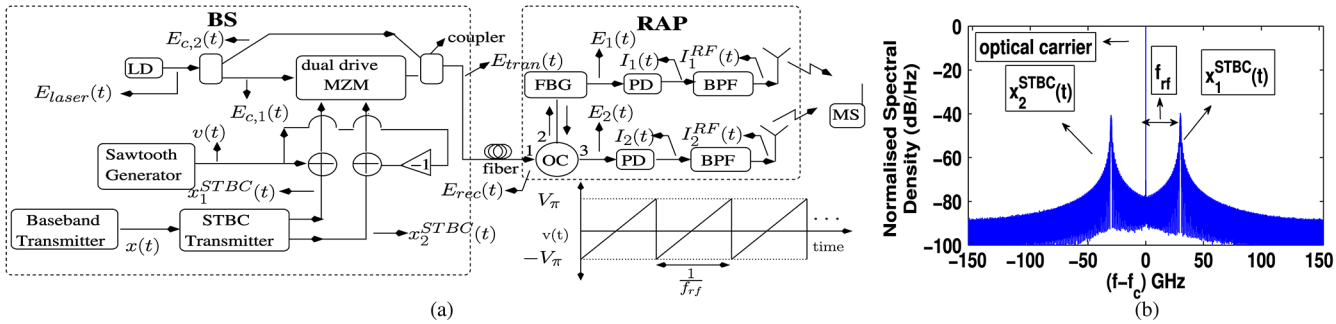

Fig. 1. (a) Proposed system architecture. (b) Spectrum of the transmitted optical signal.

Fig. 1(a) shows the temporal plot of $v(t)$. If the MZM in the BS of Fig. 1(a) has an insertion loss of t_{attn} and it is driven by voltages $V_1(t$ and $V_2(t)$, then its output optical field is

$$\begin{aligned} E_{MZM}(t) =& \frac{\sqrt{t_{attn}}}{2}\left[e^{j\frac{\pi V_1(t)}{V_\pi}} + e^{j\frac{\pi V_2(t)}{V_\pi}}\right]E_{c,1}(t) \\ =& \frac{\sqrt{t_{attn}}}{2}\left[e^{j\pi\frac{x_1^{STBC}(t)+v(t)}{V_\pi}} + e^{j\pi\frac{x_2^{STBC}(t)+v(t)}{V_\pi}}\right]E_{c,1}(t) \\ =& -\frac{\sqrt{t_{attn}}}{2}\left[e^{j\left(2\pi f_{rf}t+\pi\frac{x_1^{STBC}(t)}{V_\pi}\right)}\right. \\ & \left. + e^{j\left(-2\pi f_{rf}t+\pi\frac{x_2^{STBC}(t)}{V_\pi}\right)}\right]E_{c,1}(t). \end{aligned} \quad (4)$$

As shown in Fig. 1(a), the output of the MZM is combined with the second output $E_{c,2}(t)$ of the splitter to generate $E_{tran}(t)$. If the optical coupler's insertion loss is t_{sp}, then $E_{tran}(t)$ can be expressed from (2) and (4) as follows

$$\begin{aligned} E_{tran}(t) =& \left[-\frac{\sqrt{t_{attn}}}{2}e^{j\left(2\pi f_{rf}t+\pi\frac{x_1^{STBC}(t)}{V_\pi}\right)}\right. \\ & \left. -\frac{\sqrt{t_{attn}}}{2}e^{j\left(-2\pi f_{rf}t+\pi\frac{x_2^{STBC}(t)}{V_\pi}\right)} + 1\right]E_{LD}(t)\frac{t_{sp}}{2}. \end{aligned} \quad (5)$$

The spectrum of $E_{tran}(t)$ is shown in Fig. 1(b), where it can be seen that $E_{tran}(t)$ is an ODSB signal, in which the upper and lower sidebands carry $x_1^{STBC}(t)$ and $x_2^{STBC}(t)$, respectively.

B. Receiver in the RAP

As shown in Fig. 1(a), the optical signal $E_{tran}(t)$ propagates through the optical fiber of length L and it is received as $E_{rec}(t)$ in the RAP. The fiber attenuates the signal and its dispersion imposes a phase shift ϕ_{disp} on the two sidebands with respect to the carrier [13]. Thus, *from* (5), the received signal becomes

$$\begin{aligned} E_{rec}(t) =& e^{\frac{\alpha}{2}L}\left[-\frac{\sqrt{t_{attn}}}{2}e^{j\left(2\pi f_{rf}t+\pi\frac{x_1^{STBC}(t)}{V_\pi}+\phi_{disp}\right)}\right. \\ & \left. -\frac{\sqrt{t_{attn}}}{2}e^{j\left(-2\pi f_{rf}t+\pi\frac{x_2^{STBC}(t)}{V_\pi}-\phi_{disp}\right)} + 1\right]E_{LD}(t)\frac{t_{sp}}{2} \end{aligned} \quad (6)$$

where α is the fiber's attenuation parameter. In the RAP of Fig. 1(a), the optical signal enters Port 1 of the optical circulator (OC) and exits from Port 2, where it encounters a fiber Bragg grating (FBG) that reflects 50% of the carrier power in addition to the complete lower sideband. These filters are similar to those employed in [14]. The reflected signal then enters Port 2 of the OC and exits from Port 3. The signal passing through the FBG and the reflected signal exiting Port 3 have optical fields of $E_1(t)$ and $E_2(t)$, which can be expressed as

$$E_1(t) = e^{\frac{\alpha}{2}L}\left[\frac{1}{\sqrt{2}} - \frac{\sqrt{t_{attn}}}{2}e^{j\left(2\pi f_{rf}t+\pi\frac{x_1^{STBC}(t)}{V_\pi}+\phi_{disp}\right)}\right]E_{LD}(t)\frac{t_{sp}}{2}, \quad (7)$$

$$E_2(t) = e^{\frac{\alpha}{2}L}\left[\frac{1}{\sqrt{2}} - \frac{\sqrt{t_{attn}}}{2}e^{j\left(-2\pi f_{rf}t+\pi\frac{x_2^{STBC}(t)}{V_\pi}-\phi_{disp}\right)}\right]E_{LD}(t)\frac{t_{sp}}{2}. \quad (8)$$

Subsequently, as seen in Fig. 1(a), $E_1(t)$ and $E_2(t)$ are photo-detected using a photo-diode (PD) of responsivity R to generate currents, which can be expressed using (1), (2), (7), and (8) as

$$\begin{aligned} I_1(t) =& R|E_1(t)|^2 = \frac{Re^{\alpha L}P_{LD}(t_{sp})^2}{2} \\ & \times\left[0.5+\frac{t_{attn}}{4} - \sqrt{\frac{t_{attn}}{2}}\cos\left(2\pi f_{rf}t+\pi\frac{x_1^{STBC}(t)}{V_\pi}+\phi_{disp}\right)\right] \end{aligned} \quad (9)$$

$$\begin{aligned} I_2(t) =& R|E_2(t)|^2 = \frac{Re^{\alpha L}P_{LD}(t_{sp})^2}{2} \\ & \times\left[0.5+\frac{t_{attn}}{4} - \sqrt{\frac{t_{attn}}{2}}\cos\left(2\pi f_{rf}t+\pi\frac{x_2^{STBC}(t)}{V_\pi}-\phi_{disp}\right)\right]. \end{aligned} \quad (10)$$

The pair of photo-detected signals $I_1(t)$ and $I_2(t)$ are then filtered using bandpass filters centered at f_{rf} Hz, as shown in Fig. 1(a), in order to generate the RF signals

$$I_1^{RF}(t) = K\cos\left(2\pi f_{rf}t + \pi\frac{x_1^{STBC}(t)}{V_\pi} + \phi_{disp}\right) \quad (11)$$

and

$$I_2^{RF}(t) = K\cos\left(2\pi f_{rf}t + \pi\frac{x_2^{STBC}(t)}{V_\pi} - \phi_{disp}\right) \quad (12)$$

where K is the amplitude of the filtered signal. The above RF signals are amplified and transmitted over the wireless link to the MS of Fig. 1(a), where they are synchronously downconverted [11]. These RF signals are phase-modulated, upconverted versions of the STBC encoded complex baseband signals $e^{j(\pi\frac{x_1^{STBC}(t)}{V_\pi}+\phi_{disp})}$ and $e^{j(\pi\frac{x_2^{STBC}(t)}{V_\pi}-\phi_{disp})}$. Fiber-dispersion rotates all the symbols by a length-dependent constant phase of ϕ_{disp}

TABLE I
PARAMETER VALUES OF THE ROF LINK

Parameter	Value	Parameter	Value
R_{bit}	32 Mbps	t_{attn}	4 dB
t_{sp}	3 dB	ϵ	30 dB
λ_c	1550 nm	L	20 km
V_π	6 V	R_L	125 Ω
		Laser linewidth	10 MHz
D	16 ps/km-nm	γ	1.2 /W/km
		I_{dark}	1 nA
α	0.2 dB/km	F_n	6 dB
R	0.8 A/W	f_{rf}	30 GHz
K_{RIN} (dBc/Hz)	-155	Divesity employed	STBC

radians, which may be considered as part of the complex-valued wireless channel and hence they are jointly estimated by the wireless channel estimation technique used at the MS. In other words, if the wireless channel transmitting $I_1^{RF}(t)$ and $I_2^{RF}(t)$ has complex coefficients of h_1 and h_2, respectively, then the channel coefficients estimated at the MS and hence employed by the STBC receiver are $h_1 e^{j\phi}$ and $h_2 e^{-j\phi}$, respectively.

A practical implementation of the proposed architecture may employ a non-ideal MZM and a non-ideal sawtooth signal. A non-ideal MZM's output is given by the nth order Bessel function [3]. These imperfections generate non-linear products like intermodulation and harmonics [3]. However, we hasten to add that these non-linear signals may be significantly suppressed by the FBG filter in the receiver and by the electronic filter after photo-detection. If needed, an additional FBG filter may also be employed after port 3 of the OC in Fig. 1(a) for suppressing these signals before photo-detection by the lower photo-diode.

III. SIMULATION RESULTS

Table I shows the system parameters employed in our simulations. The photo-detected current is given by (9) and (10) and the additional dark current I_{dark}. The relative intensity noise (RIN) power, shot noise power and thermal noise power imposed by the optical link are $\sigma^2_{RIN} = K_{RIN} I^2_{dc} \Delta f$, $\sigma^2_{shot} = 2eI_{dc}\Delta f$ and $\sigma^2_{thermal} = \frac{4k_bT}{R_L}\Delta f$, respectively [15]. Here, I_{dc} is the average photo-detected current, Δf is the optical receiver's bandwidth, k_b is the Boltzmann constant, T is the absolute temperature of 290 K, R_L is the load resistance, F_n is the optical receiver amplifier's noise figure, while e is the charge of an electron. Optical propagation is given by

$$\frac{\partial A}{\partial z} = -\frac{\alpha}{2} - j\frac{\beta_2}{2}\frac{\partial^2 A}{\partial T^2} + j\gamma\left\{|A|^2 A\right\} \qquad (13)$$

where $A(z,T)$ is the envelope (or amplitude) of the modulated optical carrier after it has propagated through z km of SSMF, while $D = -\frac{2\pi c}{\lambda_c^2}\beta_2$, γ and α are the fiber's dispersion parameter, non-linearity parameter and attenuation parameter, respectively. Equation (13) was simulated using the split step Fourier method [15].

Equation (4) assumes an ideal MZM having an extinction ratio ϵ[1] of infinity in the transmitter. However, we have

[1]Extinction-ratio is defined as the ratio of the optical power transmitted for bit 1 to the power transmitted for bit 0 [15].

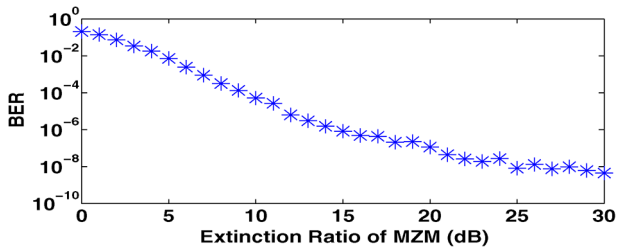

Fig. 2. System performance when employing a non-ideal MZM in transmitter.

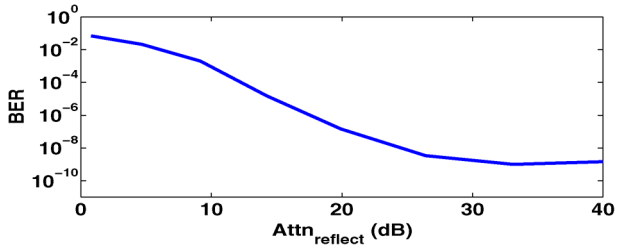

Fig. 3. System performance for non-ideal optical filtering in receiver.

$E_{MZM}(t) = \frac{\sqrt{t_{attn}}}{2}[e^{j\frac{\pi V_1(t)}{V_\pi}} + \gamma_{ext} e^{j\frac{\pi V_2(t)}{V_\pi}}]E_{c,1}(t)$ for a practical MZM, where $\gamma_{ext} = (\sqrt{\epsilon}-1)/(\sqrt{\epsilon}+1)$. Based on the discussions in Section II, we arrive at

$$I_1^{RF}(t) = K\cos\left(2\pi f_{rf} t + \pi\frac{x_1^{STBC}(t)}{V_\pi} + \phi_{disp}\right) \qquad (14)$$

and

$$I_2^{RF}(t) = K\gamma_{ext}\cos\left(2\pi f_{rf} t + \pi\frac{x_2^{STBC}(t)}{V_\pi} - \phi_{disp}\right). \qquad (15)$$

In other words, the two STBC signals that are transmitted from the RAP are not exactly of the same power, thereby resulting in a BER degradation. Fig. 2 shows the BER degradation for various extinction ratios. The simulation results shown in Fig. 2 relied on a transmit power that results in a BER of 10^{-8} for a near-ideal extinction ratio of 30 dB. It can be seen from Fig. 2 that the degradation is lower than an order of magnitude for commercially available MZMs having extinction ratios of about 20 dB.

The derivation of (11) and (12) assumed having an FBG filter in the receiver that perfectly reflected one of the sidebands, while transmitting the other. Let us now *study* the effect of employing a realistic, practical FBG filter that assumes an imperfect reflection of the sideband. Fig. 3 shows the BER degradation for various attenuation levels $Attn_{reflect}$ of the reflected sideband w.r.t. the transmitted sideband, where the ideal complete reflection of the reflected sideband corresponds to an attenuation of ∞ dB. The simulation results shown in Fig. 3 assume an ideal MZM in the transmitter in order to study the BER degradation imposed by the receiver alone. It can be seen from Fig. 3 that the BER degradation is lower than an order of magnitude for the typical attenuations of commercially available FBG filters.

The classical ODSB signal generated by employing a MZM biased at $V_\pi/2$ volts carries a single signal using both sidebands [13]. Naturally, fiber dispersion attenuates the photo-detected

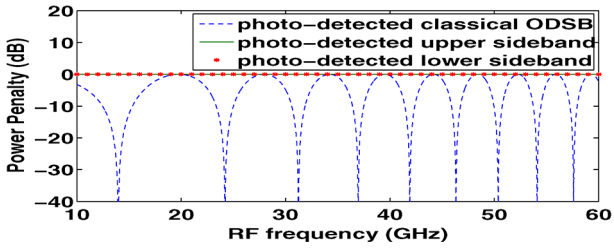

Fig. 4. System performance for various RF carriers.

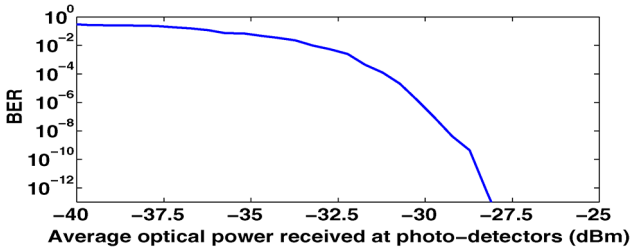

Fig. 5. BER performance of the optical link.

power of the classical chirp-free ODSB signal as per the following expression [16]

$$P_{rf} \propto \cos^2\left[\frac{\pi \cdot L \cdot D \cdot \lambda_c^2 \cdot f_{rf}^2}{c}\right] \tag{16}$$

where c is the speed of light in vacuum. This power attenuation results in a BER degradation. Fig. 4 shows the power penalty imposed on the photo-detected RF signal by fiber dispersion, where the reference is the photo-detected power for the case of no fiber dispersion. It can be seen from Fig. 4 that in the proposed scheme, the RF signals generated by the separate photo-detection of the upper and lower sidebands do not suffer from any dispersion-induced power attenuation. This is because their separate photo-detection gives the proposed scheme the advantage offered by OSSB modulation [12]. Fig. 5 shows the BER performance of the optical link proposed in this paper for the simulation parameters of Table I.

Having designed the optical link, *we now study* the performance of the overall ROF link including the wireless link. Fig. 6 shows the ideal error vector magnitude (EVM) performance of a wireless link employing STBC and no backhaul along with the EVM performance of the proposed ROF link for a laser transmit power of 0 dBm. It can be seen in Fig. 6 that the ROF backhaul imposes only negligible degradation, while enabling the designer to fully exploit the diversity gain of STBC [9]. Note that the term SNR of wireless channel in Fig. 6 refers to the SNR computed at the wireless receiver and it includes the noise added by the wireless link only.

IV. Conclusion

A ROF backhaul was conceived for supporting 2×1-element downlink STBC. Each RAP was served by an ODSB signal, each of whose sidebands carried the RF signal for one of the two STBC antennas. The downlink signal was generated by a single *MZM, where this MZM implemented* optical upconversion. This backhaul imposed negligible degradation, while enabling the exploitation of the diversity gain of STBC.

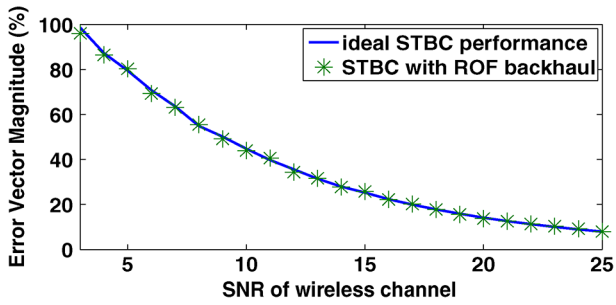

Fig. 6. Performance of wireless link relying on a ROF backhaul.

References

[1] V. Thomas, M. El-Hajjar, and L. Hanzo, "Performance improvement and cost reduction techniques for radio over fiber communications," *Commun. Surveys Tuts.*, vol. 17, no. 2, pp. 627–670, 2nd Quart. 2015.

[2] V. Thomas, M. El-Hajjar, and L. Hanzo, "Millimeter-wave radio over fiber optical upconversion techniques relying on link non-linearity," *Commun. Surveys Tuts.*, to be published. AQ3

[3] X. N. Fernando, *Radio Over Fiber for Wireless Communications: from Fundamentals to Advanced Topics*, 1st ed. Chichester, U.K.: Wiley-IEEE, 2014.

[4] G. H. Nguyen, B. Cabon, and Y. Le Guennec, "Generation of 60-GHz MB-OFDM signal-over-fiber by up-conversion using cascaded external modulators," *J. Lightw. Technol.*, vol. 27, no. 11, pp. 1496–1502, Jun. 2009.

[5] V. Thomas, S. Ghafoor, M. El-Hajjar, and L. Hanzo, "A full-duplex diversity-assisted hybrid analogue/digitized radio over fibre for optical/wireless integration," *IEEE Commun. Lett.*, vol. 17, no. 2, pp. 409–412, Feb. 2013.

[6] V. Thomas, M. El-Hajjar, and L. Hanzo, "Simultaneous optical phase and intensity modulation transmits independent signals in radio over fiber communication," *IEEE Commun. Lett.*, vol. 19, no. 4, pp. 557–560, Apr. 2015.

[7] Z. Jia, J. Yu, G. Ellinas, and G. K. Chang, "Key enabling technologies for optical-wireless networks: optical millimeter-wave generation, wavelength reuse, and architecture," *J. Lightw. Technol.*, vol. 25, no. 11, pp. 3452–3471, Nov. 2007.

[8] P. Cao *et al.*, "Photonic generation of 3-D UWB Signal using a dual-drive Mach–Zehnder modulator," *IEEE Photon. Technol. Lett.*, vol. 26, no. 14, pp. 1434–1437, Jul. 2014.

[9] S. Alamouti, "A simple transmit diversity technique for wireless communications," *IEEE J. Sel. Areas Commun.*, vol. 16, no. 8, pp. 1451–1458, Oct. 1998.

[10] I. Amiri, S. Alavi, N. Fisal, A. Supa'at, and H. Ahmad, "All-optical generation of two IEEE 802.11n signals for 2 × 2 MIMO-RoF via MRR system," *IEEE Photon. J.*, vol. 6, no. 6, pp. 1–11, Dec. 2014.

[11] L. Hanzo, S. X. Ng, T. Keller, and W. Webb, *Quadrature Amplitude Modulation*, 2nd ed. Chichester, U.K.: Wiley-IEEE Press, 2004.

[12] G. Smith, D. Novak, and Z. Ahmed, "Technique for optical SSB generation to overcome dispersion penalties in fibre-radio systems," *Electron. Lett.*, vol. 33, no. 1, pp. 74–75, Jan. 1997.

[13] J. Corral, J. Marti, and J. Fuster, "General expressions for IM/DD dispersive analog optical links with external modulation or optical up-conversion in a Mach–Zehnder electrooptical modulator," *IEEE Trans. Microw. Theory Techn.*, vol. 49, no. 10, pp. 1968–1976, Oct. 2001.

[14] A. Nirmalathas, D. Novak, C. Lim, and R. Waterhouse, "Wavelength reuse in the WDM optical interface of a millimeter-wave fiber-wireless antenna base station," *IEEE Trans. Microw. Theory Techn.*, vol. 49, no. 10, pp. 2006–2012, Oct. 2001.

[15] G. P. Agrawal, *Fiber-optic communication systems*, 4th ed. Hoboken, NJ, USA: Wiley, 2002.

[16] G. Smith and D. Novak, "Broad-band millimeter-wave (38 GHz) fiber-wireless transmission system using electrical and optical SSB modulation to overcome dispersion effects," *IEEE Photon. Technol. Lett.*, vol. 10, no. 1, pp. 141-143, Jan. 1998.

AUTHOR QUERIES

AUTHOR PLEASE ANSWER ALL QUERIES

AQ1 = Please provide keywords.
AQ2 = Please check and confirm if provided affilliation and email of all authors are correct.
AQ3 = Please provide publication update in Ref. [2].

END OF ALL QUERIES